

Rotation curves of luminous spiral galaxies

I.A. Yegorova,^{1,*} A. Babic², P. Salucci², K. Spekkens³ and A. Pizzella^{4,5}

¹ ESO Chile, Alonso de Cordova 3107, Santiago 19001, Chile

² SISSA International School for Advanced Studies, via Bonomea 265, 34136 Trieste, Italy

³ Department of Physics, Royal Military College of Canada, P.O. Box 17000, Stn Forces, Kingston, Ontario, Canada

⁴ Dipartimento di Astronomia, Università di Padova, vicolo dell'Osservatorio 3, I-35122 Padova, Italy

⁵ INAF, Osservatorio Astronomico di Padova, Padova, Italy

The dates of receipt and acceptance should be inserted later

Key words galaxies: kinematics and dynamics – galaxies: spiral – galaxies: structure

We have investigated the stellar light distribution and the rotation curves of high-luminosity spiral galaxies in the local Universe. The sample contains 30 high-quality extended $H\alpha$ and $H I$ rotation curves. The stellar disk scale-length of these objects was measured or taken from the literature. We find that in the outermost parts of the stellar disks of these massive objects, the rotation curves agree with the Universal Rotation Curve (Salucci et al. 2007), however a few rotation curves of the sample show a divergence.

© 0000 WILEY-VCH Verlag GmbH & Co. KGaA, Weinheim

1 Introduction

Rotation curves (RCs) of spiral galaxies, if unperturbed, to a very good approximation indicate the galaxy's circular velocity profile $V(R) = (Rd\Phi/dR)^{1/2}$, where Φ is the Newtonian gravitational potential and $V^2(R) = V_D^2(R) + V_H^2(R)$ is the quadratic sum of the disk and halo contributions (e.g. Salucci et al. 2011). In combination with surface photometry, they provide the mass distribution in spirals.

It is well known that the distribution of stellar light in a spiral galaxy with characteristic radius $R_{\text{opt}} \equiv 3.2R_D$, where R_D is the Freeman exponential thin disk scale-length, does not match the distribution of the gravitating matter (Bosma & van der Kruit 1979; Rubin et al. 1980; Persic & Salucci 1990). To frame this phenomenon it is helpful to define the following reference radius R_{opt} of the stellar disk: i) it is proportional to the disk scale-length, that represents the stellar distribution (Freeman 1970); ii) it encloses 83% of the total disk mass. Moreover, at R_{opt} , the disk contribution $V_D(R)$ to the circular velocity is declining rapidly. Assuming, without loss of generality, that $V_D(R) \propto R^{\nabla_D(R)}$, (where ∇ is the logarithmic slope) in any spiral we have: $\nabla_D(2.2/3.2 R_{\text{opt}}) = 0$, $\nabla_D(R_{\text{opt}}) = -0.27$, $\nabla_D(1.2 R_{\text{opt}}) \simeq -0.5$.

Then at $R \simeq R_{\text{opt}}$, V_D rapidly becomes Keplerian. Furthermore, if at $\simeq R_{\text{opt}}$ the stellar component dominates the total gravitational potential, the resulting RC must decrease with radius in the region of $2.7R_D - 3.5R_D$ (the region that will be investigated in this paper).

The RCs of spiral galaxies show a phenomenology that has led to the concept of the *Universal Rotation Curve*

(URC). This was implicit in Rubin et al. (1985), pioneered by Persic & Salucci (1991, hereafter PS91) and set in Persic, Salucci & Stel (1996, hereafter PSS). According to this paradigm, the RCs of disk galaxies can be generally represented by $V_{\text{URC}}(R/R_D; P_i)$, i.e. by a *universal* function of normalized radius, tuned by one or more galaxy observational quantities P_i (e.g. the B-band luminosity M_B as in PS91, the I-band luminosity M_I as in PSS, or the virial mass M_{vir} as in Salucci et al. (2007, hereafter S+07). Remarkably, just one global quantity takes into account for more than 90% of the RC variance. The URC phenomenology has replaced the “flat RC” paradigm and switched the focus from the structure of “a typical galaxy” to the typical systematics of the mass structure of spirals. PS91, PSS and S+07 universal velocity functions $V_{\text{URC}}^{\text{PS91}}(R/R_D; M_B)$, $V_{\text{URC}}^{\text{PSS}}(R/R_D; M_I)$, $V_{\text{URC}}^{\text{S+07}}(R/R_D; M_{\text{vir}})$ are successive improvements of the URC paradigm. While a complete assessment of the role of minor parameters in the URC (e.g. bulge, stellar surface density) has yet to be performed, the functions V_{URC} obtained in the above studies match the kinematics of individual RCs very well. At any radius R , V_{URC} predicts the circular velocities of spirals of known luminosity and disk scale-length within an error that is one order of magnitude smaller than i) the radial variations of the RC in each object, ii) the cosmic variance in the RC amplitudes, at any fixed radius R/R_D .

An important contribution on the systematic properties of RCs has come from the work of Catinella et al. (2006, hereafter C+06). They studied 2200 RCs of disk galaxies and constructed the template RCs for objects of different luminosities. They found that RC amplitudes and slopes are, at any radius, functions of the galaxy luminosity (see Eq. (1), Table 2 and Fig. 1 in C+06). They also found that a generic spiral RC is well represented by Universal Tem-

* Corresponding author: e-mail: iyegorov@eso.org

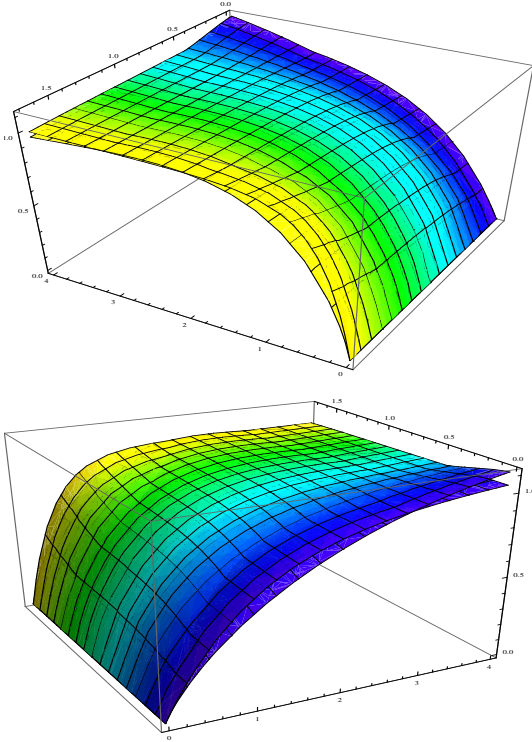


Fig. 1 Comparison between the S+07 and the C+06 Universal Rotation Curves. *Upper panel:* the representing 3-D surfaces are plotted together out to $4R_D$. We plot $V_{\text{URC}}^{\text{S+07}}(R/R_D, M_I)/V_{\text{URC}}^{\text{S+07}}(3.2, M_I)$ and $V_{\text{URC}}^{\text{C+06}}(R/R_D, M_I)/V_{\text{URC}}^{\text{C+06}}(3.2, M_I)$ as a function of radius, in units of disk scale-length (i.e. of R/R_D) and of I-magnitudes (i.e. of $(M_I - 19.4)/2.5$). Brighter colors indicate more luminous galaxies. *Lower panel:* the same surfaces of the upper panel, shown from a different angle.

plates, more specifically by a function of radius in disk scale-length units and of I-band luminosity:

$V_{\text{URC}}^{\text{C+06}}(R/R_D, M_I)$. The S+07 and C+06 URCs are compared here for the first time in Fig. 1. They coincide at low and intermediate luminosities.

However, at the high-luminosity end, $M_I < -22$, i.e. for the top 5% objects in luminosity, from $R > 2R_D$ onward, there is a discrepancy between the C+06 and the S+07 URCs. In this region, in fact, the profile of the latter slightly declines with radius, while the C+06 URC profile, on the contrary, shows a modest but clear increase with radius.

Due to the high-luminosity cut-off in the spiral galaxy luminosity function, this issue concerns a small number of objects, which however belong to the important “class” of spirals with most extreme properties in term of luminosity/mass and disk size. The analysis of these objects requires extra care with respect to the rest of the spiral population. In fact, these galaxies show an intrinsically “flattish” rotation curve, so that kinematical effects of the Grand Design spiral structure or of other not-axisymmetric motions are very evident in the RCs as wiggles and oscillations. Com-

paring “flat” (and in some cases) non-extended RCs with large observational uncertainties or non-axisymmetric velocity components (as done in C+06 and PSS) may introduce biases in the kinematical investigations.

Furthermore, for these objects, we need a very precise determination of their (flattish) RC slope in order to derive properly the underlying mass distribution. To show this, and neglecting for simplicity of argument the bulge and the HI disk components, we recall that the condition of centrifugal equilibrium is

$$V^2(R) = V_D^2(R) + V_H^2(R), \quad (1)$$

where $V(R)$ is the circular velocity we infer from the rotation curve. By defining $\nabla \equiv (\frac{d \log V(R)}{d \log R})$,

$\nabla_D(R) \equiv (\frac{d \log V_D(R)}{d \log R})$, and $\nabla_H(R)$ similarly for the halo component, and the disk fractional contribution to the RC as $\beta \equiv \frac{V_D^2(R)}{V^2(R)}$, we obtain the RC-profile equation:

$$\nabla(R) = \beta(R) \nabla_D(R) + (1 - \beta(R)) \nabla_H(R) \quad (2)$$

Eq. (2) shows that at a radius R the value of the observed logarithmic slope $\nabla(R)$ is determined by the sum of $\nabla_D(R)$ and $\nabla_H(R)$, each one weighted by the corresponding mass fraction inside R : $1 - \beta(R)$, and $\beta(R)$. We note that $\nabla_D(R)$ is known from the photometry and $\nabla_D(x)$ is equal in all galaxies for any x .

For the sake of simplicity, all quantities, when estimated at R_{opt} , drop their subscript, e.g. $\nabla \equiv \nabla(R_{\text{opt}})$. Furthermore, let us recall that, for an exponential thin disk (see Freeman 1970): $\nabla_D(2.2R_D) = 0$, $\nabla = -0.27$, and $V_D(2.2R_D) = 1.28V_D(3.2R_D)$, where $3.2R_D = R_{\text{opt}}$. Supported by observations and successful mass modeling we can assume that, between $2.2R_D$ (the radius where $dV_D/dR = 0$), and R_{opt} , both $V(R)$ and $V_H(R)$ are roughly linear (e.g. in the region considered $V(R) \simeq V_{\text{opt}}(1 + (R/R_{\text{opt}} - 1)\nabla)$). Then, Eq. (2), evaluated at $2.2R_D$ and at R_{opt} leads to the following system of equations

$$-0.27\beta + \nabla_H - \beta\nabla_H = \nabla \quad (3)$$

$$-1.71\beta\nabla_H + 2.2\frac{\nabla}{3.2 - \nabla}\nabla_H = 2.2\frac{\nabla}{3.2 - \nabla} \quad (4)$$

The value of $\nabla(R)$ ranges in spirals between $\simeq -0.3$ (corresponding to a negligible amount of dark matter (DM) inside R_{opt}), and $\simeq 1$ (corresponding to a negligible amount of luminous matter (LM) inside R_{opt}). More specifically, the population of high luminosity spirals (under study here) shows

$$-0.15 \leq \nabla \leq 0.15, \quad (5)$$

where the above range includes the values from the individual RCs of our sample, and those derived from the C+06, and S+07 URCs. The solution of Eq. (3, 4) shown in Fig. 2 is a relationship between ∇_H and β , with ∇ the known parameter. When $\nabla \simeq 0$ a precision of $\delta\nabla < 0.04$ is required to perform a proper mass modeling, since larger errors produce unacceptable uncertainties. In fact, from Fig. 2 we realize that for the value of $\nabla = 0.12$, consistent with that of

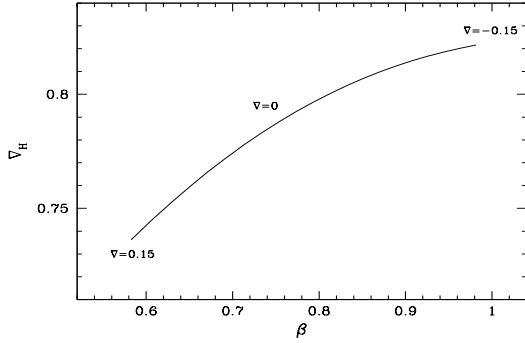


Fig. 2 β and ∇_H as a function of ∇ .

the high luminosity end of C+06 URC, we have $\nabla_H = 0.72$ and $\beta = 0.58$, values that are still reproducible (though with some difficulty) by a NFW halo + Freeman disk mass model (NFW) (Salucci & Persic 1999), while, for the value of $\nabla = -0.12$, consistent with that of the high luminosity end of the S+07 URC we have: $\nabla_H = 0.9$ and $\beta = 0.95$, values that cannot be accounted by any NFW mass model.

In building the URC at the Highest Luminosity End (HLE), one should use only reliable RCs. However only 9 HLE RCs in PSS, and not many more in C+06 are of such quality, e.g. can be used for individual mass modeling.

By inspecting the HLE RCs in the region between $2.7R_D$ and $3.5R_D$ we realize that they flatten and then, at least in some cases, start to decline. Over a limited region, centered on $\simeq 3R_D$ and $(0.5 - 0.7) R_D$ wide, $\nabla(R)$ passes from positive values ~ 0.15 , to zero and, in some cases, to also negative values down to ~ -0.15 . This RC behaviour, unique in the spiral RC phenomenology, requires that for HLE the disk scale-length R_D be known to good precision. In fact, if we underestimate its value by more than 15%, we may obtain, for a negative ∇ an incorrect positive estimate (as a consequence of measuring at $2.7R_D$ rather than at $R_{\text{opt}} \equiv 3.2R_D$).

Considering also works published after 2007, the aims of this paper are 1) to take or build from raw literature data all available/possible smoothed high quality RCs of high-luminosity spirals; 2) to measure or take from literature their disk scale-length and then, for these objects; 3) to investigate the individual RC profiles; and 4) explore the phenomenology of HLE RCs.

2 Data selection

We select high-quality RCs of HLE late-type spirals (Sb or later) that satisfy the following criteria:

1. the objects are at the high end of the spiral luminosity/velocity range: $220 \text{ km/s} < V(R_{\text{opt}}) < 335 \text{ km/s}$ (corresponding to $-22.4 < M_B < -20.6$);
2. the inclination i of the galaxies is $57^\circ < i < 90^\circ$, ensuring sufficiently small error in the normalization of the RC;

3. the RCs have a good spatial resolution: the distance between two consecutive velocity measurements must be $\leq 0.5 R_D$;
4. the RCs are sufficiently well-sampled: at least 4 independent RC points lie in the region of interest: $2 < R/R_D < 4$;
5. the RCs are unperturbed, ensuring that they reflect the gravitational potential. Moreover, they do not exhibit features indicative of prominent spiral structure nor warps;
6. the RCs have small observational uncertainties in their amplitudes and derivatives: $\delta V/V < 0.04$, $\delta \nabla < 0.05$, in order to ensure a sufficient precision in the determination of $\nabla(R)$.

These criteria are just those necessary to: a) identify the objects that we want to study, and b) ensure that we obtain reliable RCs. No result of this paper depends critically on this (very reasonable) selection process.

3 The disk scale-length

A reliable estimate of the disk scale-length R_D is fundamental in the sample selection. Looking at the samples of potential RCs, we must notice that in Vogt et al. (2004) and C+06 samples the available R_D were derived from I-band imaging observations of Haynes et al. (1999). The authors fitted only the outer parts of the disk, since their aim was to extrapolate the light profile beyond the outer edge and obtain the total magnitude to use in establishing the Tully-Fisher relation. For the objects in the Courteau (1996) sample, the available R_D were obtained from exponential fits to the radial r-band surface brightness profile, performed over the region $50 - 90\%$ of the radius at $26 \text{ mag arcsec}^{-2}$, again over the outer disk region. These determinations of R_D based on outer surface brightness data is certainly biased and often incorrect. The proper analysis requires that the latter be decomposed in the separate contributions of a bulge and a disk and that, obviously, the whole data are taken into account. Among several drawbacks that the former procedure can have, we draw the attention to the following a) due to extinction, especially in inclined galaxies, surface brightness profile will steepen towards the outer edge, and the scale-length measured in the outer disk will be smaller than the scale-length measured over the whole disk; b) to neglect the bulge can affect the values of the disk scale-length in an unpredictable way.

Thus, for 15 candidate objects in the above samples we opted to re-derive the disk scale-lengths from available near-infrared images, by using the two-dimensional disk-bulge decomposition code GALFIT (Peng et al. 2002). All the images are taken from the K_s -band 2MASS All Sky Release Atlas. They were photometrically calibrated, and the typical FWHM for the point-spread function (PSF) is $\sim 3''$. Two components were used in the fits: an exponential disk and a Sérsic bulge or a PSF for unresolved central sources. For

a number of objects, the bulge half-light radius is comparable to the PSF FWHM, and the corresponding r_e estimates should be considered unreliable. In Fig. 3 we show an example of a successful two dimensional image decomposition, and in Fig. 4 we show the corresponding one-dimensional surface brightness profiles. The derived disk scale-lengths R_D are reported in the Table 1 and marked with an asterisk.

The new disk scale-lengths values tend to differ by 10% to 50% from those in C+06, Vogt et al. (2004) and Courteau (1996). In 5 cases the new (larger) scale-lengths made the available RC not extended enough to be included in the sample (see Table 2, we report these values since they could be useful in future studies). Of course, we also found in the literature properly determined disk scale-lengths, that we have adopted in our studies (see Table 1).

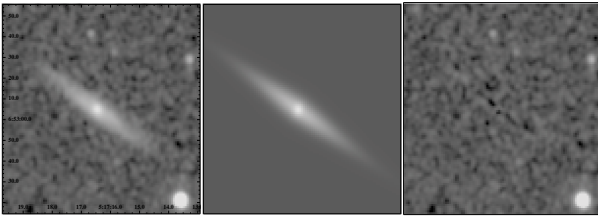


Fig. 3 Two-dimensional 2MASS K_s -band image decomposition for UGC 3279. From left to right: the original image, the model image, and the residual image.

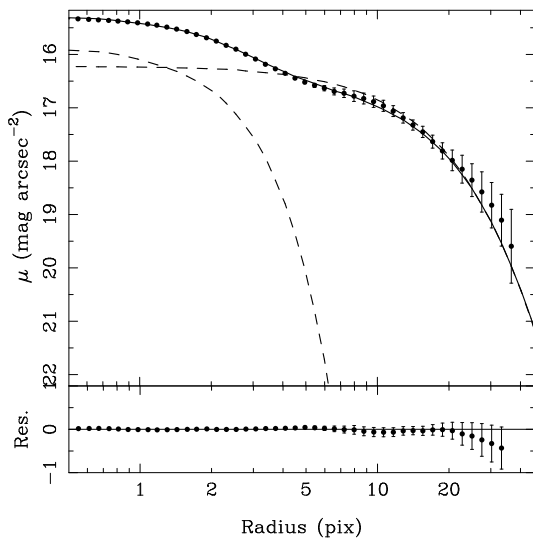


Fig. 4 Surface brightness profile of UGC 3279. The image profile is marked by filled circles, the complete model (obtained from 2-D image decomposition) with a solid line, and the disk-bulge components of the model are marked with dashed lines. The model-data residuals are also shown in the bottom panel.

4 The Sample

At the end of the selection procedure we have a sample of 30 *high-quality* RCs of HLE spirals (see Table 1). In detail we have: 1) $H\alpha$ RCs: 2 from Courteau (1997), 9 from Vogt et al. (2004), 5 from C+06, 1 from Blais-Ouellette (2006), and 8 from PSS. 2) HI RCs¹: 2 from Spekkens et al. (2006), 2 from Kregel & van der Kruit (2004); Kregel, van der Kruit & Freeman (2005) and 1 from Corbelli et al. (2010).

Let us stress that a number of published RCs (including also some in PSS and in C+06) did not enter the present sample since they are not 1) extended, or 2) smooth, 3) symmetric, or 4) of sufficient spatial resolution, or 5) with small velocity r.m.s. We believe that these requirements are essential to investigate ∇ in HLE spirals.

This is the largest sample of high-luminosity spirals ever studied in which every object has suitable kinematics and photometry. Unfortunately, the number of objects is still limited and the results obtained must be considered as indications. Let us stress that, at this point in time, this is the best we can do: there are additional high luminosity objects with kinematical data in the literature, but they do not satisfy the criteria for inclusion in our sample (e.g. UGC 8707 (Courteau 1997) and UGC 1901, AGC 250022 (C+06)).

5 The Rotation Curves

The 30 raw RCs have been binned as in Yegorova & Salucci (2007), i.e. smoothed with respect to non-axisymmetric motions and observational errors. We adopted radial bins sizes of $0.2R_D$ and $0.6R_D$ for $H\alpha$ and HI RCs, respectively. We plot the RCs in the Appendix.

We do not consider here the innermost regions of the RCs, some dominated by a bulge, and we plot RCs only for $R > R_D$. In a small number of cases, the contribution from the central bulge to the dynamics of the galaxy is not negligible. At this radius this does not affect the present results, in that, at larger radii these RCs are very similar to the others. However, an analysis like this one for spirals with more significant bulges is certainly worthy of future attention. In the website indicated in Salucci et al. (2011) the whole 30 RC data are available for download.

We focus on the behavior of the RCs near R_{opt} . We compute the logarithmic slope ∇ by fitting linearly the RC in the neighborhood of R_{opt} . The logarithmic slope ∇ is estimated within an uncertainty of about 0.05. We therefore, define a (slowly) declining RC when $\nabla(R_{opt}) \leq -0.05$, a flat RC when $-0.05 \leq \nabla(R_{opt}) \leq 0.05$ and a rising RC when $0.05 \leq \nabla(R_{opt})$.

We find that at R_{opt} 40% of the RCs are declining, 50% flat and 10% slowly rising. However, there are cases when

¹ The RCs from Spekkens et al. (2006) combine both $H\alpha$ and HI data. But since the kinematics in the region of interest ($R > R_D$) are covered by the HI component, we consider them as HI RCs for the purposes of this study.

Table 1 Data: the absolute B magnitude are calculated using the apparent B-magnitude from HyperLeda database. Distance: is taken from the NED NASA database. Reference: Vogt et al. (2004) - 1, Courteau (1997) - 2, C+06 - 3, Kregel & van der Kruit (2004); Kregel, van der Kruit & Freeman (2005) - 4, Blais-Ouellette et al. (2006) - 5, Spekkens et al. (2006) - 6, PSS - 7, Corbelli et al. (2010) - 8.

Name	M_B (mag)	Inc ($^\circ$)	∇	Distance (Mpc)	R_D (kpc)	Data	Ref
UGC944	-21.37	81	-0.15	68.5	2.9	$H\alpha$	1
UGC1076	-22.08	72	-0.05	179	5.5*	$H\alpha$	3
UGC1094	-20.97	80	-0.13	61.6	3.4	$H\alpha$	1
UGC3279	-21.92	82	0.21	114	5.4*	$H\alpha$	1
UGC4895	-20.82	70	0.01	96.1	3.5	$H\alpha$	1
UGC4941	-22.37	83	0.03	83.2	3.0	$H\alpha$	1
UGC8140	-21.0	78	-0.02	97.4	4.8	$H\alpha$	1
UGC8220	-21.14	86	-0.04	97.7	4.5*	$H\alpha$	1
UGC9805	-21.13	68	-0.02	47.3	3.3*	$H\alpha$	3
UGC10692	-21.47	77	-0.25	130	8.6	$H\alpha$	3
UGC10815	-20.77	78	0.01	54.9	4.0*	$H\alpha$	2
UGC10981	-21.84	66	-0.16	151	5.1*	$H\alpha$	1
UGC11455	-21.81	84	0.1	76.8	2.2	HI	6
UGC11527	-20.63	78	-0.08	77.2	3.5*	$H\alpha$	3
UGC12200	-21.49	57	0.01	136	3.8*	$H\alpha$	2
UGC12678	-21.28	90	-0.03	127	5.2*	$H\alpha$	1
AGC241056	-22.08	80	-0.02	293	8.0*	$H\alpha$	3
NGC1247	-21.81	90	-0.12	53.4	4.8	$H\alpha$	7
NGC5170	-20.89	90	-0.11	19.1	6.5	HI	4
NGC5985	-21.4	58	-0.08	36.7	5.3	$H\alpha$	5
NGC7300	-21.48	72	-0.04	68.1	4.4	$H\alpha$	7
IC2974	-21.8	86	-0.13	76.9	5.5	$H\alpha$	7
ESO141-G20	-21.98	90	-0.07	59.9	4.5	$H\alpha$	7
ESO141-G34	-21.65	90	-0.02	59.1	5.3	$H\alpha$	7
ESO240-G11	-21.41	90	-0.01	38.3	9.1	HI	4
ESO350-G23	-21.56	77	0.05	21.4	4.3	$H\alpha$	7
ESO374-G27	-21.60	62	-0.1	122	5.5	$H\alpha$	7
ESO563-G21	-22.0	83	0.04	59.9	2.0	HI	6
ESO601-G9	-22.37	90	0.03	37	5.4	$H\alpha$	7
M31	-21.71	77	0.04	-	4.5	HI	8

a “rising” RC (at R_{opt}), shows a decline farther out (e.g. ESO350-G23).

It is evident that adopting an incorrect value for $R_{\text{opt}} \simeq 3.2R_D$ would bias the analysis. When the adopted R_{opt} is smaller than the actual one, the error leads to a wrong positive estimate of $\nabla(R_{\text{opt}})$ (since $V(R)$ in the neighborhood of R_{opt} turns over and begins to decline). When instead the adopted R_{opt} is larger than the actual one, the resulting value of $\nabla(R_{\text{opt}})$ is (roughly) correct since the HLE RCs for $R > R_{\text{opt}}$ are already converged to a linear/flat profile). Thus, adopting the C+06 disk scale-lengths leads to an increase in fraction of (apparently) rising RC’s. This, with the fact that some rising RC do exist, explains the noted discrepancy between the S+07 and C+06.

We plot the RCs of our sample all together in Fig. 5. They are normalized by setting $V(R_{\text{opt}}) = 250$ km/s in each galaxy, with the normalized velocity curve defined as $250 V(R)/V(R_{\text{opt}})$ km/s. This specific value was adopted for visual clarity and comparison of RCs with different $V(R_{\text{opt}})$.

We overplot (with red and black dashed lines, see Fig. 5) the URC *profile* corresponding to $V(R_{\text{opt}}) = 220$ km/s and $V(R_{\text{opt}}) = 350$ km/s as given by S+07. We note that the URC, in general, well represents the individual profiles, but there are notable exceptions in which we detect a rising RCs (e.g. UGC 3279, UGC 11455).

6 Discussion

We have investigated the RCs of high-luminosity spirals, a class of objects whose kinematical properties had not yet been thoroughly examined so far. The sample consists of 30 high-quality, extended $H\alpha$ and HI rotation curves with $220 \text{ km/s} \leq V(R_{\text{opt}}) \leq 335 \text{ km/s}$ that represent, in this paper, the HLE spirals. We found that, *to a first approximation*, HLE have a mass distribution that follows the same phenomenology of spirals of smaller mass.

We proved this by examining and studying each RC individually. We determined that the discrepancy *at the high-luminosity end* between the S+07 URC and the C+06 URC

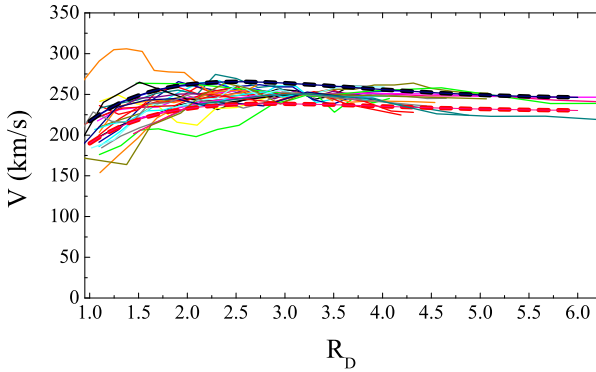


Fig. 5 The RCs of the sample normalized to the same $V(R_{\text{opt}})$. The dashed red and black lines indicate the URC predictions for $V(R_{\text{opt}}) = 220$ km/s and $V(R_{\text{opt}}) = 350$ km/s correspondingly.

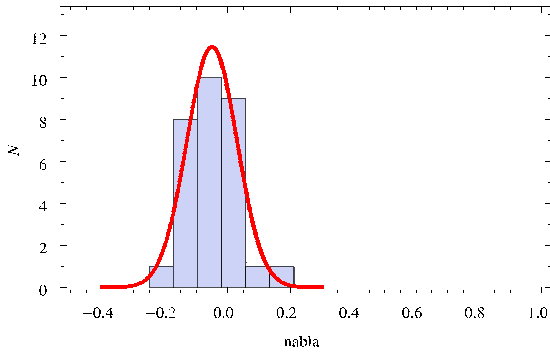


Fig. 6 Histogram of the values of ∇ 's for the objects of our sample, compared with the predictions of the S+07 URC (red solid line).

originates from differences in the way that scale-lengths are estimated in these two studies. Nevertheless, in partial agreement with C+06, a presumably *small* fraction of HLE spirals with gently rising RC out to R_{opt} seems to exist. The individual study of these objects will be very important.

At R_{opt} , the radius where the velocity profile of the luminous components starts to decrease, the RCs of our sample divide between declining, flat, and (a few) mildly rising RCs.

Let us compare the distribution of ∇ 's as found in the present sample with the one that comes from the S+07 URC predictions, i.e. a Gaussian centered at $\nabla = -0.05$ with width of 0.1 (see Fig. 6). They are in a very good agreement considering that, in principle, ∇ can take *any* value between -0.5 and 1 . In general, HLE RCs seem to be in agreement with the S+07 URC.

Most of the RCs of our sample exhibit a clear decline at some radius $R > 2 R_D$ indicating that the stellar disk contributes to the mass budget in this regime. However, in all cases $\nabla > \nabla_D \simeq -0.27$, which implies the presence of a dark matter halo.

Although to derive the properties of the dark and luminous matter in HLE requires their individual mass modeling, some important feature can still be obtained, also from a simpler RC analysis. By means of the equations shown in the Introduction we obtain that at R_{opt} : 1) $0.7 \leq \beta \leq 0.9$ i.e. high luminosity objects are luminous matter dominated, and 2) without any loss of generality, the halo density profile can be written as $\rho_H(R) \propto R^{2(\nabla_H - 2)}$, therefore the density slope emerges being very shallow $0.77 \leq \nabla_H \leq 0.82$.

As in spirals of lower luminosities (see PSS), we do not see any “cosmic conspiracy”, i.e. any fine-tuning among the values of P_i describing the DM/LM distributions (the halo core radius and the central density, and the disk mass) that “creates” the observed “flattish” RC profile. On the contrary, the RCs of high luminosity spirals show quite large ranges in the values of the P_i , that, instead, turn out to be very correlated. The uncertainty ranges are relevant, they indicate the existence of a real variance of the mass distribution of HLE (as represented by our sample).

The framework of a NFWD requires $\nabla(R) > 0.05 \simeq 0.1$ from $1 R_D$ to $6 R_D$ (see Salucci & Persic 1999). This prediction is not fulfilled by the RC profiles of our spirals: many of them, *decline* i.e. have $\nabla(R) < 0$, over > 1 disk scale-length (see Table 1 and Fig. 6). Therefore, also in high luminosity galaxies, a disagreement between *naive* Λ CDM predictions and the actual data does clearly emerge.

We conclude this paper by indicating possible causes of the (moderate) cosmic variance of the RC profiles of HLE: effects of the environment, the presence of an active galactic nucleus, the stellar and central black hole feedback are possibilities that need to be investigated with a much larger sample of objects.

Table 2 Measured disk scale-lengths for galaxies not in final sample.

Name	M_B (mag)	R_D (kpc)
UGC562	-22.21	6.8*
UGC8017	-20.89	3.1*
AGC24797	-21.57	4.7*
AGC211561	-21.51	5.5*
AGC320581	-21.1	4.6*

Acknowledgements. We thank the anonymous referee for valuable comments that improved the paper. A.P. acknowledge funding through grants CPDA089220/08 by Padua University and ASI-INAf I/009/10/0.

References

- Blais-Ouellette, S., Amram, P., Carignan, C., Swaters, R.: 2004, *A&A* 420, 147
- Bosma, A., van der Kruit, P. C.: 1979, *A&A* 79, 281
- Catinella, B., Giovanelli, R., Haynes, M. P.: 2006, *ApJ* 640, 751 (C+06)
- Corbelli, E., Lorenzoni, S., Walterbos, R., Braun, R., Thilker, D.: 2010, *A&A*, 511A, 89
- Courteau, S.: 1996, *ApJS* 103, 363
- Courteau, S.: 1997, *AJ* 114, 2402
- Freeman, K. C.: 1970, *ApJ* 160, 811
- Haynes, M.P., Giovanelli, R., Salzer, J. J., Wegner, G., Freudling, W., da Costa, L. N., Herter, T., Vogt, N. P.: 1999, *AJ*, 117, 1668
- Kregel, M., van der Kruit, P. C.: 2004, *MNRAS* 352, 787
- Kregel, M., van der Kruit, P. C., Freeman, K. C.: 2005, *MNRAS* 358, 503
- Peng, C. Y., Ho, L. C., Impey, C. D., Rix, H. W.: 2002, *AJ* 124, 266
- Persic, M., Salucci, P.: 1990, *MNRAS* 247, 349
- Persic, M., Salucci, P.: 1991, *ApJ* 368, 60 (PS91)
- Persic, M., Salucci, P., Stel, F.: 1996, *MNRAS* 281, 27 (PSS)
- Rubin, V. C., Burstein, D., Ford, W. K., Jr, Thonnard, N.: 1985, *ApJ* 289, 81
- Rubin, V. C., Ford, W. K. Jr, Thonnard, N.: 1980, *ApJ* 238, 471
- Salucci, P., Frigerio Martins Ch., Lapi, A.: 2011, preprint (arXiv:1102.1184)
- Salucci, P., Lapi, A., Tonini, C., Gentile, G., Yegorova, I., Klein, U.: 2007, *MNRAS* 378, 41 (S+07)
- Salucci, P., Persic, M.: 1999, *A&A* 351, 44
- Spekkens, K., Giovanelli, R.: 2006, *AJ* 132, 1426
- Vogt, N. P., Haynes, M. P., Herter, T., Giovanelli, R.: 2004, *AJ* 127, 3273
- Yegorova, I., Salucci, P.: 2007, *MNRAS* 377, 507

A RCs of the sample

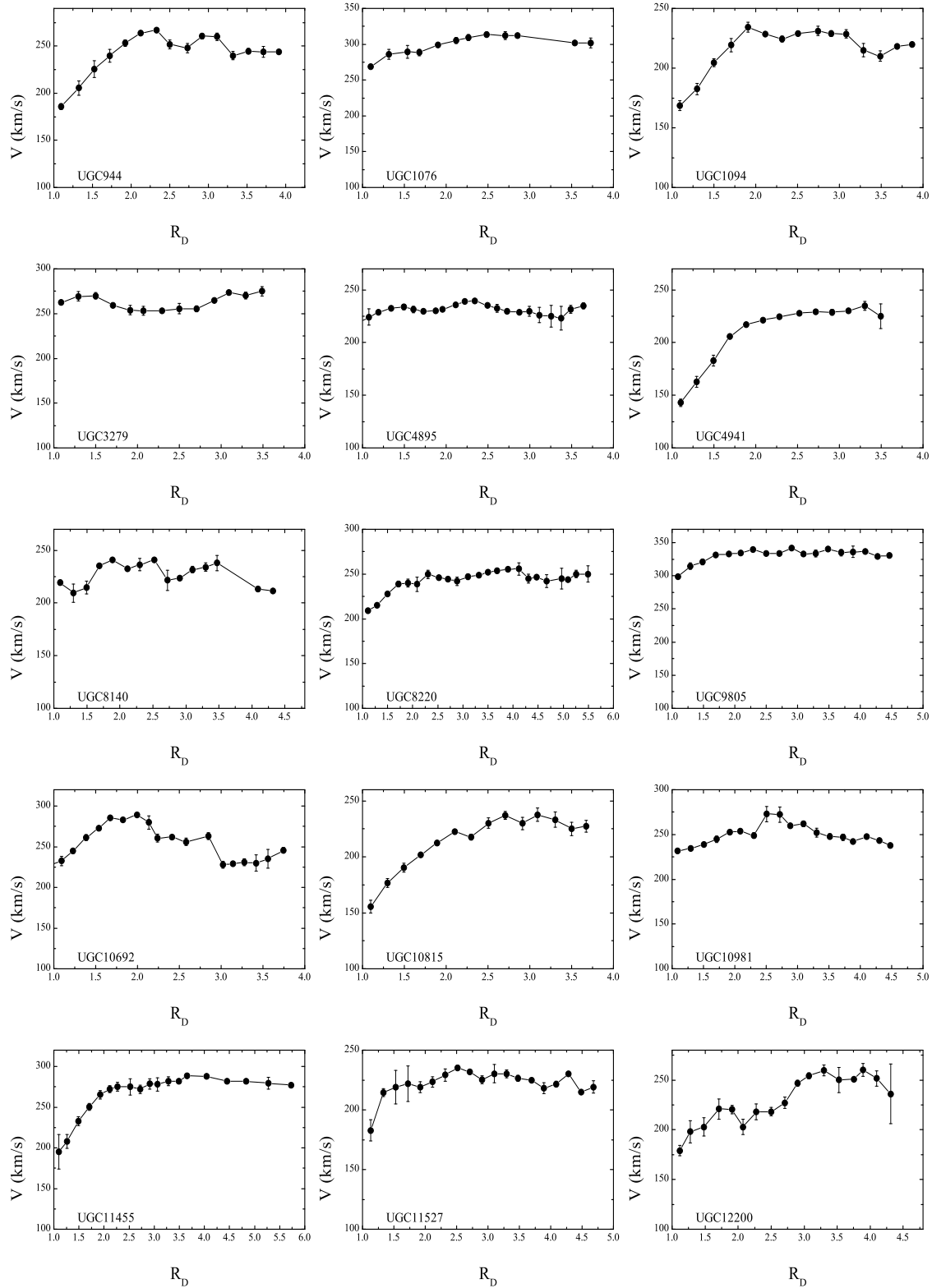


Fig. A1 RCs from our sample.

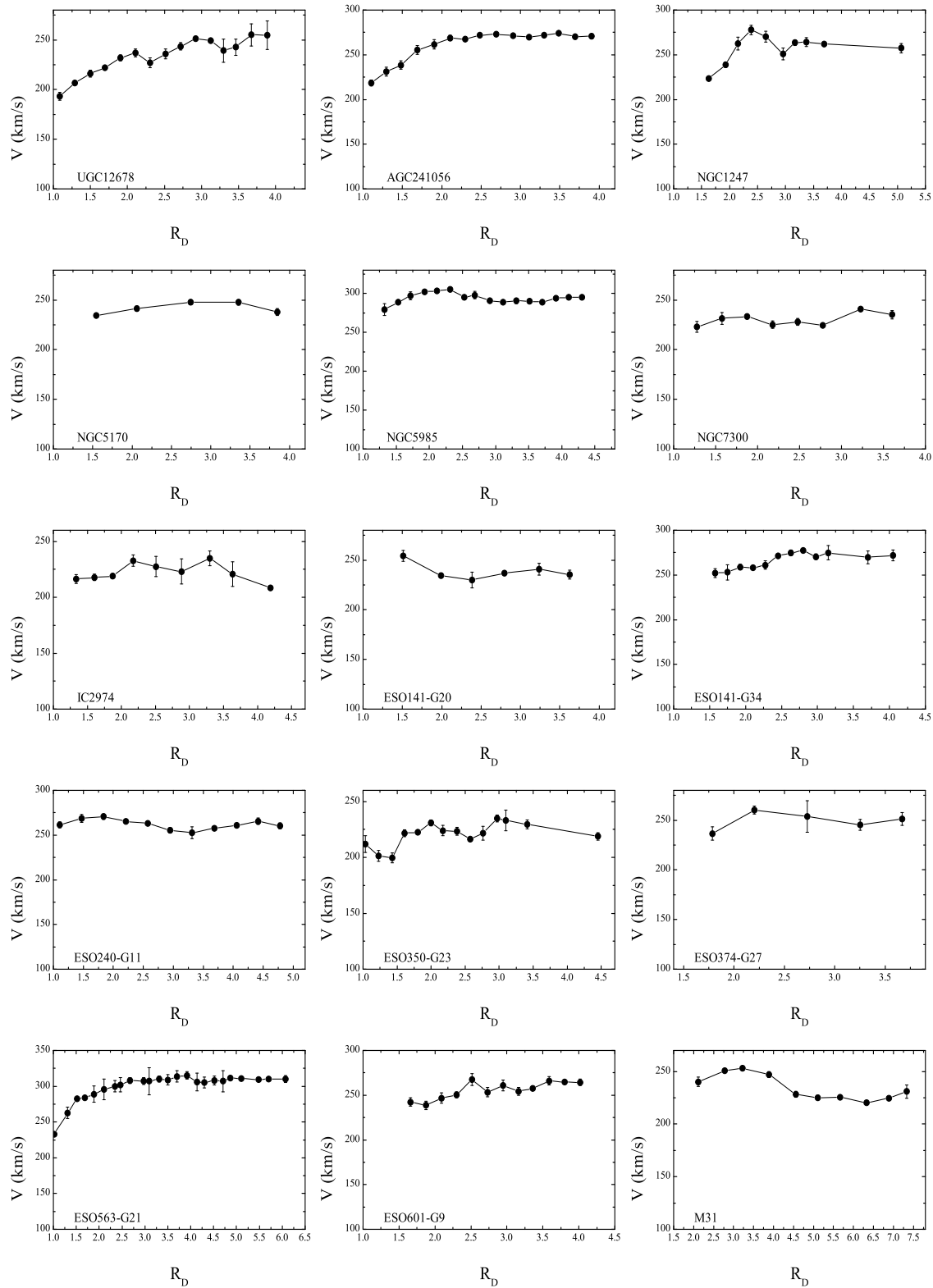


Fig. A2 RCs from our sample.